

Linearised Optimal Transport Distances

Dynamics and Discretization: PDEs, Sampling, and Optimization
Simons Programme on Geometric Methods in Optimization and Sampling

Matthew Thorpe

Joint Work with Tianji Cai (University of California Santa Barbara), Junyi Cheng (University of California Santa Barbara) and Bernhard Schmitzer (TU Munich)

Department of Mathematics
University of Manchester

27th October 2021



The Wasserstein distance is *great* as a distance between signals/images, because...

- ① Lagrangian modelling,
- ② simple to understand compared to other Lagrangian methods such as large deformation diffeomorphic metric mapping,
- ③ metric properties (in particular symmetry).
- ④ geodesics and Riemannian structure,
- ⑤ theoretical and characterising properties such as existence of optimal transport maps and optimal transport plans (under appropriate conditions).

The Wasserstein distance is *great* as a distance between signals/images, because...

- 1 Lagrangian modelling,
- 2 simple to understand compared to other Lagrangian methods such as large deformation diffeomorphic metric mapping,
- 3 metric properties (in particular symmetry).
- 4 geodesics and Riemannian structure,
- 5 theoretical and characterising properties such as existence of optimal transport maps and optimal transport plans (under appropriate conditions).

But,...

- 1 it places restrictive conditions on the input, in particular signals have to be probability measures,
- 2 computationally expensive (despite recent advances),
- 3 there is a lack of off-the-shelf data analysis tools.

Motivation

The Wasserstein distance is *great* as a distance between signals/images, because...

- 1 Lagrangian modelling,
- 2 simple to understand compared to other Lagrangian methods such as large deformation diffeomorphic metric mapping,
- 3 metric properties (in particular symmetry).
- 4 geodesics and Riemannian structure,
- 5 theoretical and characterising properties such as existence of optimal transport maps and optimal transport plans (under appropriate conditions).

But,...

- 1 it places restrictive conditions on the input, in particular signals have to be probability measures,
- 2 computationally expensive (despite recent advances),
- 3 there is a lack of off-the-shelf data analysis tools.

Solution: **linearise an unbalanced optimal transport metric!**

Balanced Optimal Transport

Let $\mu, \nu \in \mathcal{P}(\Omega)$. The Wasserstein distance can be defined in one of three ways.

Balanced Optimal Transport

Let $\mu, \nu \in \mathcal{P}(\Omega)$. The Wasserstein distance can be defined in one of three ways.

① Monge formulation:

$$d_W^2(\mu, \nu) := \inf_{T: T_{\#}\mu = \nu} \int_{\Omega} |x - T(x)|^2 d\mu(x);$$

Balanced Optimal Transport

Let $\mu, \nu \in \mathcal{P}(\Omega)$. The Wasserstein distance can be defined in one of three ways.

- 1 Monge formulation:

$$d_W^2(\mu, \nu) := \inf_{T: T_{\#}\mu = \nu} \int_{\Omega} |x - T(x)|^2 d\mu(x);$$

- 2 Kantorovich formulation:

$$d_W^2(\mu, \nu) := \min_{\pi \in \Pi(\mu, \nu)} \int_{\Omega \times \Omega} |x - y|^2 d\pi(x, y);$$

Balanced Optimal Transport

Let $\mu, \nu \in \mathcal{P}(\Omega)$. The Wasserstein distance can be defined in one of three ways.

① Monge formulation:

$$d_W^2(\mu, \nu) := \inf_{T: T\#\mu=\nu} \int_{\Omega} |x - T(x)|^2 d\mu(x);$$

② Kantorovich formulation:

$$d_W^2(\mu, \nu) := \min_{\pi \in \Pi(\mu, \nu)} \int_{\Omega \times \Omega} |x - y|^2 d\pi(x, y);$$

③ Benamou–Brenier formulation:

$$d_W^2(\mu, \nu) := \inf \left\{ \int_0^1 \int_{\Omega} \left\| \frac{d\omega_t}{d\rho_t}(x) \right\|^2 d\rho_t(x) dt : (\rho, \omega) \in \mathcal{CE}(\mu, \nu) \right\}$$

where

$$(\rho, \omega) \in \mathcal{CE}(\mu, \nu) \Leftrightarrow \frac{\partial \rho}{\partial t} + \nabla_x \omega = 0, \rho_0 = \mu, \rho_1 = \nu.$$

Balanced Optimal Transport

Let $\mu, \nu \in \mathcal{P}(\Omega)$. The Wasserstein distance can be defined in one of three ways.

① Monge formulation:

$$d_{\text{W}}^2(\mu, \nu) := \inf_{T: T_{\#}\mu = \nu} \int_{\Omega} |x - T(x)|^2 d\mu(x);$$

② Kantorovich formulation:

$$d_{\text{W}}^2(\mu, \nu) := \min_{\pi \in \Pi(\mu, \nu)} \int_{\Omega \times \Omega} |x - y|^2 d\pi(x, y);$$

③ Benamou–Brenier formulation:

$$d_{\text{W}}^2(\mu, \nu) := \inf \left\{ \int_0^1 \int_{\Omega} \left\| \frac{d\omega_t}{d\rho_t}(x) \right\|^2 d\rho_t(x) dt : (\rho, \omega) \in \mathcal{CE}(\mu, \nu) \right\}$$

where

$$(\rho, \omega) \in \mathcal{CE}(\mu, \nu) \Leftrightarrow \frac{\partial \rho}{\partial t} + \nabla_x \omega = 0, \rho_0 = \mu, \rho_1 = \nu.$$

Under appropriate conditions all three are equivalent.

The Riemannian Structure of Wasserstein Spaces

① Let $v_t = \frac{d\omega_t}{d\rho_t}$, then

$$d_W^2(\mu, \nu) = \int_0^1 \int_{\Omega} \|v_t(x)\|^2 d\rho_t(x) dt.$$

The Riemannian Structure of Wasserstein Spaces

- ① Let $v_t = \frac{d\omega_t}{d\rho_t}$, then

$$d_W^2(\mu, \nu) = \int_0^1 \int_{\Omega} \|v_t(x)\|^2 d\rho_t(x) dt.$$

- ② $T_t^* = tT^* + (1-t)\text{Id}$ is the maps the geodesic, i.e.
 $\mu_t = [T_t^*]_{\#}\mu$ is the geodesic between μ and ν .

The Riemannian Structure of Wasserstein Spaces

- ① Let $v_t = \frac{d\omega_t}{d\rho_t}$, then

$$d_W^2(\mu, \nu) = \int_0^1 \int_{\Omega} \|v_t(x)\|^2 d\rho_t(x) dt.$$

- ② $T_t^* = tT^* + (1-t)\text{Id}$ is the maps the geodesic, i.e. $\mu_t = [T_t^*]_{\#}\mu$ is the geodesic between μ and ν .
- ③ Moreover $v_t \circ T_t^* = T^* - \text{Id}$ and

$$\int_{\Omega} \|v_t(x)\|^2 d\rho_t(x) = \int_{\Omega} \|v_0\|^2 d\mu(x)$$

for all $t \in [0, 1]$.

The Riemannian Structure of Wasserstein Spaces

- ① Let $v_t = \frac{d\omega_t}{d\rho_t}$, then

$$d_W^2(\mu, \nu) = \int_0^1 \int_{\Omega} \|v_t(x)\|^2 d\rho_t(x) dt.$$

- ② $T_t^* = tT^* + (1-t)\text{Id}$ is the maps the geodesic, i.e. $\mu_t = [T_t^*]_{\#}\mu$ is the geodesic between μ and ν .
- ③ Moreover $v_t \circ T_t^* = T^* - \text{Id}$ and

$$\int_{\Omega} \|v_t(x)\|^2 d\rho_t(x) = \int_{\Omega} \|v_0\|^2 d\mu(x)$$

for all $t \in [0, 1]$.

- ④ Hence $d_W^2(\mu, \nu) = \int_{\Omega} \|v_0\|^2 d\mu(x)$.

The Riemannian Structure of Wasserstein Spaces

- ① Let $v_t = \frac{d\omega_t}{d\rho_t}$, then

$$d_W^2(\mu, \nu) = \int_0^1 \int_{\Omega} \|v_t(x)\|^2 d\rho_t(x) dt.$$

- ② $T_t^* = tT^* + (1-t)\text{Id}$ is the maps the geodesic, i.e. $\mu_t = [T_t^*]_{\#}\mu$ is the geodesic between μ and ν .
- ③ Moreover $v_t \circ T_t^* = T^* - \text{Id}$ and

$$\int_{\Omega} \|v_t(x)\|^2 d\rho_t(x) = \int_{\Omega} \|v_0\|^2 d\mu(x)$$

for all $t \in [0, 1]$.

- ④ Hence $d_W^2(\mu, \nu) = \int_{\Omega} \|v_0\|^2 d\mu(x)$.
- ⑤ Let $g_W(\mu; u, v) = \int_{\Omega} u \cdot v d\mu$, then

$$d_W^2(\mu, \nu) = g_W(\mu; v_0, v_0).$$

The Linear Wasserstein Distance

1 Let $\text{Log}_W(\mu; \nu) = \nu_0$, so

$$d_W(\mu, \nu) = \|\text{Log}_W(\mu; \nu)\|_{L^2(\mu)}.$$

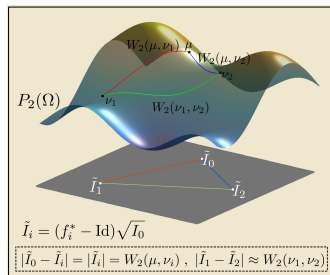


Figure credit: Soheil Kolouri.

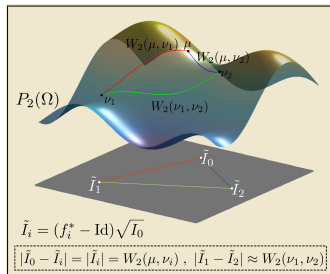
The Linear Wasserstein Distance

- 1 Let $\text{Log}_W(\mu; \nu) = \nu_0$, so

$$d_W(\mu, \nu) = \|\text{Log}_W(\mu; \nu)\|_{L^2(\mu)}.$$

- 2 Now (following Wang, Slepčev, Basu, Ozolek and Rohde (2013)) we define

$$d_{W,\mu,\text{lin}}(\mu_1, \mu_2) = \|\text{Log}_W(\mu; \mu_1) - \text{Log}_W(\mu; \mu_2)\|_{L^2(\mu)}.$$



The Linear Wasserstein Distance

- 1 Let $\text{Log}_W(\mu; \nu) = \nu_0$, so

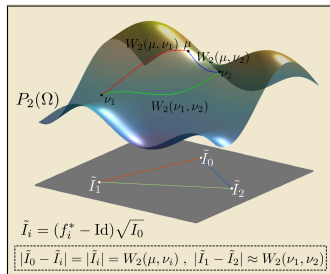
$$d_W(\mu, \nu) = \|\text{Log}_W(\mu; \nu)\|_{L^2(\mu)}.$$

- 2 Now (following Wang, Slepčev, Basu, Ozolek and Rohde (2013)) we define

$$d_{W,\mu,\text{lin}}(\mu_1, \mu_2) = \|\text{Log}_W(\mu; \mu_1) - \text{Log}_W(\mu; \mu_2)\|_{L^2(\mu)}.$$

- 3 Linear embedding map:

$$P_{W,\mu,\text{lin}}(\mu_i) = \text{Log}_W(\mu; \mu_i).$$



The Linear Wasserstein Distance

- 1 Let $\text{Log}_W(\mu; \nu) = \nu_0$, so

$$d_W(\mu, \nu) = \|\text{Log}_W(\mu; \nu)\|_{L^2(\mu)}.$$

- 2 Now (following Wang, Slepčev, Basu, Ozolek and Rohde (2013)) we define

$$d_{W,\mu,\text{lin}}(\mu_1, \mu_2) = \|\text{Log}_W(\mu; \mu_1) - \text{Log}_W(\mu; \mu_2)\|_{L^2(\mu)}.$$

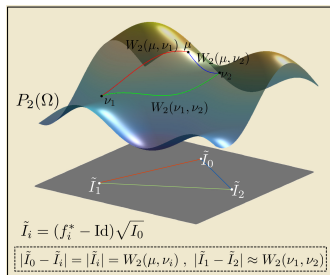
- 3 Linear embedding map:

$$P_{W,\mu,\text{lin}}(\mu_i) = \text{Log}_W(\mu; \mu_i).$$

- 4 **Linear Optimal Transport Assumption:**

$$d_W(\mu_1, \mu_2) \approx d_{W,\mu,\text{lin}}(\mu_1, \mu_2) = \|P_{W,\mu,\text{lin}}(\mu_1) - P_{W,\mu,\text{lin}}(\mu_2)\|_{L^2(\mu)}.$$

Figure credit: Soheil Kolouri.



Approximate Numerical Method

- 1 Solve the Kantorovich formulation to find π^* (e.g. Sinkhorn's algorithm)

$$d_W^2(\mu, \nu) := \min_{\pi \in \Pi(\mu, \nu)} \int_{\Omega \times \Omega} |x - y|^2 d\pi(x, y).$$

- 2 Extract T^* the optimal Monge map from $\pi^* = (\text{Id} \times T^*)_{\#}\mu$

$$d_W^2(\mu, \nu) := \inf_{T: T_{\#}\mu = \nu} \int_{\Omega} |x - T(x)|^2 d\mu(x).$$

- 3 Compute the velocity map at time $t = 0$, i.e. $v_0 = T^* - \text{Id}$

$$d_W^2(\mu, \nu) = \int_{\Omega} \|v_0\|^2 d\mu(x).$$

Road map:

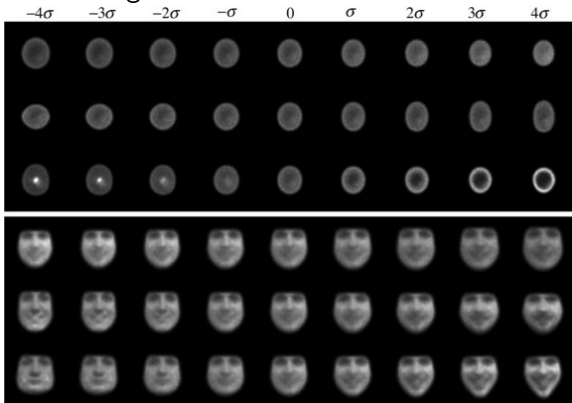
$$\nu \quad \mapsto \quad \pi^* \quad \mapsto \quad T^* \quad \mapsto \quad v_0.$$

Transport Based Morphometry

Example Data:



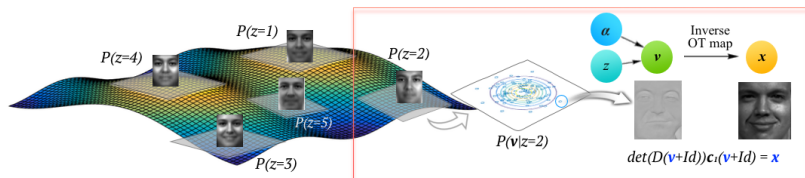
Principle Component Analysis on Linear Embedding:



Source: Wang, Slepčev, Basu, Ozolek and Rohde, *A Linear Optimal Transportation Framework for Quantifying and Visualizing Variations in Sets of Images*, International Journal of Computer Vision 101(2):254–269, 2013.

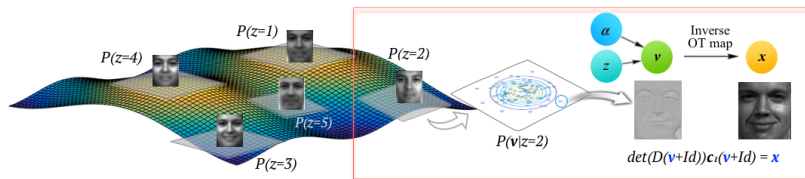
Data Generating

- Aim:** Generate new data points from the Wasserstein manifold of images.



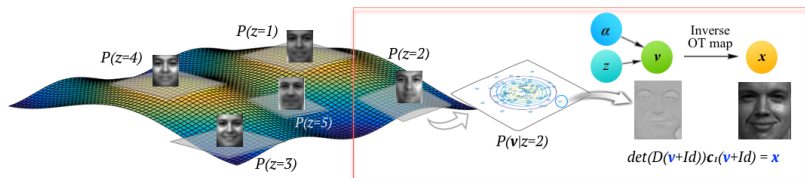
Data Generating

- 1 **Aim:** Generate new data points from the Wasserstein manifold of images.
- 2 **Idea:** Approximate the manifold at K -points.



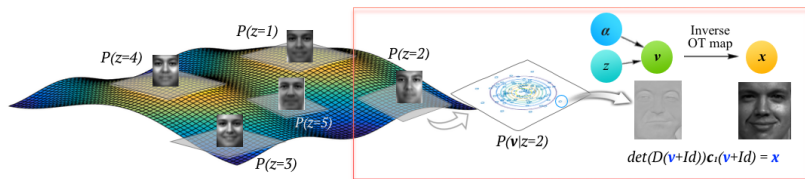
Data Generating

- 1 **Aim:** Generate new data points from the Wasserstein manifold of images.
- 2 **Idea:** Approximate the manifold at K -points.
- 3 **Strategy:**



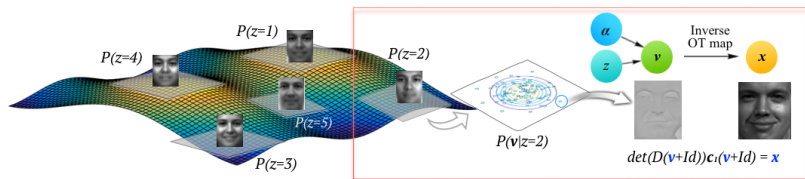
Data Generating

- 1 **Aim:** Generate new data points from the Wasserstein manifold of images.
- 2 **Idea:** Approximate the manifold at K -points.
- 3 **Strategy:**
 - 1 Cluster the data $\{\mu_i\}_{i=1}^n$ into K groups.



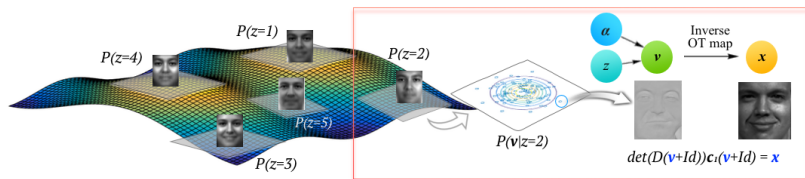
Data Generating

- 1 **Aim:** Generate new data points from the Wasserstein manifold of images.
- 2 **Idea:** Approximate the manifold at K -points.
- 3 **Strategy:**
 - 1 Cluster the data $\{\mu_i\}_{i=1}^n$ into K groups.
 - 2 For each cluster find the centre ν_k which will define the K points we approximate the manifold by.



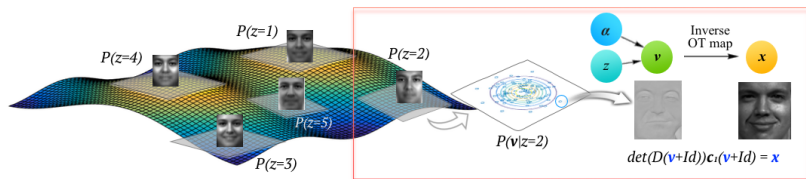
Data Generating

- 1 **Aim:** Generate new data points from the Wasserstein manifold of images.
- 2 **Idea:** Approximate the manifold at K -points.
- 3 **Strategy:**
 - 1 Cluster the data $\{\mu_i\}_{i=1}^n$ into K groups.
 - 2 For each cluster find the centre ν_k which will define the K points we approximate the manifold by.
 - 3 At each of the K centres model the tangent space by a Gaussian with mean m_k and covariance W_k .



Data Generating

- 1 **Aim:** Generate new data points from the Wasserstein manifold of images.
- 2 **Idea:** Approximate the manifold at K -points.
- 3 **Strategy:**
 - 1 Cluster the data $\{\mu_i\}_{i=1}^n$ into K groups.
 - 2 For each cluster find the centre ν_k which will define the K points we approximate the manifold by.
 - 3 At each of the K centres model the tangent space by a Gaussian with mean m_k and covariance W_k .
 - 4 To generate a new data point (i) sample a cluster centre $k \in \{1, \dots, K\}$, then (ii) sample a tangent vector $v \sim N(m_k, W_k)$, finally (iii) create a new image by pushing forward the cluster centre ν_k by the transport map $T = v + \text{Id}$.



Are we Learning New Images?



- 1 Top row, all 19 original images.
- 2 Second and third rows, generated images.

Source: Park and T., *Representing and Learning High Dimensional Data with the Optimal Transport Map from a Probabilistic Viewpoint*, CVPR, 2018.

- 1 Recall the continuity equation:

$$(\rho, \omega) \in \mathcal{CE}(\mu, \nu) \Leftrightarrow \frac{\partial \rho}{\partial t} + \nabla_x \omega = 0, \rho_0 = \mu, \rho_1 = \nu.$$

- 1 Recall the continuity equation:

$$(\rho, \omega) \in \mathcal{CE}(\mu, \nu) \Leftrightarrow \frac{\partial \rho}{\partial t} + \nabla_x \omega = 0, \rho_0 = \mu, \rho_1 = \nu.$$

- 2 We now consider the continuity equation with source:

$$(\rho, \omega, \zeta) \in \mathcal{CES}(\mu, \nu) \Leftrightarrow \frac{\partial \rho}{\partial t} + \nabla_x \omega = \zeta, \rho_0 = \mu, \rho_1 = \nu.$$

- 1 Recall the continuity equation:

$$(\rho, \omega) \in \mathcal{CE}(\mu, \nu) \Leftrightarrow \frac{\partial \rho}{\partial t} + \nabla_x \omega = 0, \rho_0 = \mu, \rho_1 = \nu.$$

- 2 We now consider the continuity equation with source:

$$(\rho, \omega, \zeta) \in \mathcal{CES}(\mu, \nu) \Leftrightarrow \frac{\partial \rho}{\partial t} + \nabla_x \omega = \zeta, \rho_0 = \mu, \rho_1 = \nu.$$

- 3 The Kondratyev, Monsaingeon and Vorotnikov (2016), Chizat, Peyré, Schmitzer and Vialard (2018, 2018a), and Liero, Mielke and Savaré (2018) model:

$$\int_0^1 \int_{\Omega} \left(\frac{d\zeta_t}{d\rho_t}(x) \right)^2 d\rho_t(x) dt.$$

Unbalanced Optimal Transport via Benamou–Brenier

- 1 Recall the continuity equation:

$$(\rho, \omega) \in \mathcal{CE}(\mu, \nu) \Leftrightarrow \frac{\partial \rho}{\partial t} + \nabla_x \omega = 0, \rho_0 = \mu, \rho_1 = \nu.$$

- 2 We now consider the continuity equation with source:

$$(\rho, \omega, \zeta) \in \mathcal{CES}(\mu, \nu) \Leftrightarrow \frac{\partial \rho}{\partial t} + \nabla_x \omega = \zeta, \rho_0 = \mu, \rho_1 = \nu.$$

- 3 The Kondratyev, Monsaingeon and Vorotnikov (2016), Chizat, Peyré, Schmitzer and Vialard (2018, 2018a), and Liero, Mielke and Savaré (2018) model:

$$\int_0^1 \int_{\Omega} \left(\frac{d\zeta_t}{d\rho_t}(x) \right)^2 d\rho_t(x) dt.$$

- 4 The Hellinger–Kantorovich distance:

$$d_{\text{HK}}^2(\mu, \nu) := \inf_{(\rho, \omega, \zeta) \in \mathcal{CES}(\mu, \nu)} \int_0^1 \int_{\Omega} \left(\left\| \frac{d\omega_t}{d\rho_t} \right\|^2 + \frac{1}{4} \left(\frac{d\zeta_t}{d\rho_t} \right)^2 \right) d\rho_t dt.$$

- ① Let KL be the Kullback–Leibler divergence

$$\text{KL}(\mu|\nu) = \int \varphi\left(\frac{d\mu}{d\nu}\right) d\nu$$

if $\mu \ll \nu$ and where $\varphi(s) = s \log(s) - s + 1$.

Soft Marginal Kantorovich Form

- 1 Let KL be the Kullback–Leibler divergence

$$\text{KL}(\mu|\nu) = \int \varphi\left(\frac{d\mu}{d\nu}\right) d\nu$$

if $\mu \ll \nu$ and where $\varphi(s) = s \log(s) - s + 1$.

- 2 Let

$$c(x, y) = \begin{cases} -2 \log(\cos \|x - y\|) & \text{if } \|x - y\| < \frac{\pi}{2} \\ +\infty & \text{else.} \end{cases}$$

Soft Marginal Kantorovich Form

- 1 Let KL be the Kullback–Leibler divergence

$$\text{KL}(\mu|\nu) = \int \varphi\left(\frac{d\mu}{d\nu}\right) d\nu$$

if $\mu \ll \nu$ and where $\varphi(s) = s \log(s) - s + 1$.

- 2 Let

$$c(x, y) = \begin{cases} -2 \log(\cos \|x - y\|) & \text{if } \|x - y\| < \frac{\pi}{2} \\ +\infty & \text{else.} \end{cases}$$

- 3 Then, (Liero, Mielke and Saveré (2018))

$$d_{\text{HK}}^2(\mu, \nu) = \inf_{\pi \in \mathcal{M}_+(\Omega^2)} \left\{ \int_{\Omega^2} c d\pi + \text{KL}(P_{1\#}\pi|\mu) + \text{KL}(P_{2\#}\pi|\nu) \right\}.$$

Soft Marginal Kantorovich Form

- 1 Let KL be the Kullback–Leibler divergence

$$\text{KL}(\mu|\nu) = \int \varphi\left(\frac{d\mu}{d\nu}\right) d\nu$$

if $\mu \ll \nu$ and where $\varphi(s) = s \log(s) - s + 1$.

- 2 Let

$$c(x, y) = \begin{cases} -2 \log(\cos \|x - y\|) & \text{if } \|x - y\| < \frac{\pi}{2} \\ +\infty & \text{else.} \end{cases}$$

- 3 Then, (Liero, Mielke and Saveré (2018))

$$d_{\text{HK}}^2(\mu, \nu) = \inf_{\pi \in \mathcal{M}_+(\Omega^2)} \left\{ \int_{\Omega^2} c d\pi + \text{KL}(P_{1\#}\pi|\mu) + \text{KL}(P_{2\#}\pi|\nu) \right\}.$$

- 4 Furthermore, there exists π^* , T^* and $\tilde{\mu}$ such that $\pi^* = (\text{Id} \times T^*)_{\#}\tilde{\mu}$ is optimal.

P A R E N T A L
A D V I S O R Y
E X P L I C I T C O N T E N T

Warning: Long (and uninformative) equations are present on the next slide.

Hellinger–Kantorovich Geodesics via Optimal Plans

Let $\mu, \nu \in \mathcal{M}_+(\Omega)$, π^* optimal and T^* be the Monge map $\pi^* = (\text{Id} \times T^*)_{\#} \tilde{\mu}$. Let $\tilde{\mu} = P_{1\#} \pi^*$, $\tilde{\nu} = P_{2\#} \pi^*$ and write

$$\mu = u\tilde{\mu} + \mu^\perp \qquad \nu = w\tilde{\nu} + \nu^\perp.$$

Then a geodesic is given by

$$\begin{aligned} \tilde{\rho}_t &= X \left(t; \cdot, u(\cdot), T^*(\cdot), w \circ T^*(\cdot) \right)_{\#} \left[M \left(t; \cdot, u(\cdot), T^*(\cdot), w \circ T^*(\cdot) \right) \tilde{\mu} \right] \\ \rho_t &= \tilde{\rho}_t + (1-t)^2 \mu^\perp + t^2 \nu^\perp \\ \omega_t &= X \left(t; \cdot, u(\cdot), T^*(\cdot), w \circ T^*(\cdot) \right)_{\#} \left[M \left(t; \cdot, u(\cdot), T^*(\cdot), w \circ T^*(\cdot) \right) \frac{\partial X}{\partial t} \left(t; \cdot, u(\cdot), T^*(\cdot), w \circ T^*(\cdot) \right) \tilde{\mu} \right] \\ \tilde{\zeta}_t &= X \left(t; \cdot, u(\cdot), T^*(\cdot), w \circ T^*(\cdot) \right)_{\#} \left[\frac{\partial M}{\partial t} \left(t; \cdot, u(\cdot), T^*(\cdot), w \circ T^*(\cdot) \right) \tilde{\mu} \right] \\ \zeta_t &= \tilde{\zeta}_t - 2(1-t)\mu^\perp + 2t\nu^\perp. \end{aligned}$$

where

$$\begin{aligned} M(t) &= (1-t)^2 m_0 + t^2 m_1 + 2t(1-t)\sqrt{m_0 m_1} \cos \|x_0 - x_1\| \\ \varphi(t) &= \cos^{-1} \left(\frac{(1-t)\sqrt{m_0} + t\sqrt{m_1} \cos(\|x_0 - x_1\|)}{\sqrt{M(t)}} \right) \\ X(t) &= x_0 + \frac{x_1 - x_0}{\|x_0 - x_1\|} \varphi(t). \end{aligned}$$

Time Independent Benamou–Brenier Form

Thm: Let $\mu, \nu \in \mathcal{M}_+(\Omega)$ and $\pi^* = (\text{Id} \times T^*)_{\#} \tilde{\mu}$ be optimal. Let (ρ, ω, ζ) be the geodesics constructed on the previous slide. Set for $t \in [0, 1)$:

$$\mathbf{v}_t = \frac{d\omega_t}{d\rho_t} \qquad \alpha_t = \frac{d\tilde{\zeta}_t}{d\rho_t} - 2(1-t) \frac{d\mu^\perp}{d\rho_t}.$$

Time Independent Benamou–Brenier Form

Thm: Let $\mu, \nu \in \mathcal{M}_+(\Omega)$ and $\pi^* = (\text{Id} \times T^*)_{\#} \tilde{\mu}$ be optimal. Let (ρ, ω, ζ) be the geodesics constructed on the previous slide. Set for $t \in [0, 1)$:

$$v_t = \frac{d\omega_t}{d\rho_t} \quad \alpha_t = \frac{d\tilde{\zeta}_t}{d\rho_t} - 2(1-t) \frac{d\mu^\perp}{d\rho_t}.$$

Then

$$v_0(x) = \begin{cases} \frac{T^*(x)-x}{\|T^*(x)-x\|} \sqrt{\frac{w(T^*(x))}{u(x)}} \sin(\|T^*(x)-x\|) & \tilde{\mu}\text{-a.e.}, \\ 0 & \mu^\perp\text{-a.e.}, \end{cases}$$
$$\alpha_0(x) = \begin{cases} 2 \left(\sqrt{\frac{w(T^*(x))}{u(x)}} \cos(\|T^*(x)-x\|) - 1 \right) & \tilde{\mu}\text{-a.e.}, \\ -2 & \mu^\perp\text{-a.e.} \end{cases}$$

Time Independent Benamou–Brenier Form

Thm: Let $\mu, \nu \in \mathcal{M}_+(\Omega)$ and $\pi^* = (\text{Id} \times T^*)_{\#} \tilde{\mu}$ be optimal. Let (ρ, ω, ζ) be the geodesics constructed on the previous slide. Set for $t \in [0, 1)$:

$$v_t = \frac{d\omega_t}{d\rho_t} \quad \alpha_t = \frac{d\tilde{\zeta}_t}{d\rho_t} - 2(1-t) \frac{d\mu^\perp}{d\rho_t}.$$

Then

$$v_0(x) = \begin{cases} \frac{T^*(x)-x}{\|T^*(x)-x\|} \sqrt{\frac{w(T^*(x))}{u(x)}} \sin(\|T^*(x)-x\|) & \tilde{\mu}\text{-a.e.}, \\ 0 & \mu^\perp\text{-a.e.}, \end{cases}$$
$$\alpha_0(x) = \begin{cases} 2 \left(\sqrt{\frac{w(T^*(x))}{u(x)}} \cos(\|T^*(x)-x\|) - 1 \right) & \tilde{\mu}\text{-a.e.}, \\ -2 & \mu^\perp\text{-a.e.} \end{cases}$$

and

$$d_{\text{HK}}^2(\mu, \nu) = \int_{\Omega} \left(\|v_0\|^2 + \frac{1}{4}(\alpha_0)^2 \right) d\mu + \|\nu^\perp\|.$$

Linear Hellinger–Kantorovich Distance

- 1 One can show that $\tilde{\mu}, \mu^\perp \perp \nu^\perp$, so $\mu \perp \nu^\perp$.

Linear Hellinger–Kantorovich Distance

- ① One can show that $\tilde{\mu}, \mu^\perp \perp \nu^\perp$, so $\mu \perp \nu^\perp$.
- ② In particular, if $\text{spt}(\mu) = \Omega$ then $\nu^\perp = 0$, and

$$d_{\text{HK}}^2(\mu, \nu) = \int_{\Omega} \left(\|v_0\|^2 + \frac{1}{4}(\alpha_0)^2 \right) d\mu.$$

Linear Hellinger–Kantorovich Distance

- 1 One can show that $\tilde{\mu}, \mu^\perp \perp \nu^\perp$, so $\mu \perp \nu^\perp$.
- 2 In particular, if $\text{spt}(\mu) = \Omega$ then $\nu^\perp = 0$, and

$$d_{\text{HK}}^2(\mu, \nu) = \int_{\Omega} \left(\|v_0\|^2 + \frac{1}{4}(\alpha_0)^2 \right) d\mu.$$

- 3 Let $\text{Log}_{\text{HK}}(\mu; \nu) = (v_0, \alpha_0)$, so

$$d_{\text{HK}}(\mu, \nu) = \|\text{Log}_{\text{HK}}(\mu; \nu)\|_{L^2(\mu)}.$$

Linear Hellinger–Kantorovich Distance

- 1 One can show that $\tilde{\mu}, \mu^\perp \perp \nu^\perp$, so $\mu \perp \nu^\perp$.
- 2 In particular, if $\text{spt}(\mu) = \Omega$ then $\nu^\perp = 0$, and

$$d_{\text{HK}}^2(\mu, \nu) = \int_{\Omega} \left(\|v_0\|^2 + \frac{1}{4}(\alpha_0)^2 \right) d\mu.$$

- 3 Let $\text{Log}_{\text{HK}}(\mu; \nu) = (v_0, \alpha_0)$, so

$$d_{\text{HK}}(\mu, \nu) = \|\text{Log}_{\text{HK}}(\mu; \nu)\|_{L^2(\mu)}.$$

- 4 Now we define

$$d_{\text{HK}, \mu, \text{lin}}(\mu_1, \mu_2) = \|\text{Log}_{\text{HK}}(\mu; \mu_1) - \text{Log}_{\text{HK}}(\mu; \mu_2)\|_{L^2(\mu)}.$$

Linear Hellinger–Kantorovich Distance

- 1 One can show that $\tilde{\mu}, \mu^\perp \perp \nu^\perp$, so $\mu \perp \nu^\perp$.
- 2 In particular, if $\text{spt}(\mu) = \Omega$ then $\nu^\perp = 0$, and

$$d_{\text{HK}}^2(\mu, \nu) = \int_{\Omega} \left(\|v_0\|^2 + \frac{1}{4}(\alpha_0)^2 \right) d\mu.$$

- 3 Let $\text{Log}_{\text{HK}}(\mu; \nu) = (v_0, \alpha_0)$, so

$$d_{\text{HK}}(\mu, \nu) = \|\text{Log}_{\text{HK}}(\mu; \nu)\|_{L^2(\mu)}.$$

- 4 Now we define

$$d_{\text{HK}, \mu, \text{lin}}(\mu_1, \mu_2) = \|\text{Log}_{\text{HK}}(\mu; \mu_1) - \text{Log}_{\text{HK}}(\mu; \mu_2)\|_{L^2(\mu)}.$$

- 5 Linear embedding map:

$$P_{\text{HK}, \mu, \text{lin}}(\mu_i) = \text{Log}_{\text{HK}}(\mu; \mu_i).$$

Linear Hellinger–Kantorovich Distance

- 1 One can show that $\tilde{\mu}, \mu^\perp \perp \nu^\perp$, so $\mu \perp \nu^\perp$.
- 2 In particular, if $\text{spt}(\mu) = \Omega$ then $\nu^\perp = 0$, and

$$d_{\text{HK}}^2(\mu, \nu) = \int_{\Omega} \left(\|v_0\|^2 + \frac{1}{4}(\alpha_0)^2 \right) d\mu.$$

- 3 Let $\text{Log}_{\text{HK}}(\mu; \nu) = (v_0, \alpha_0)$, so

$$d_{\text{HK}}(\mu, \nu) = \|\text{Log}_{\text{HK}}(\mu; \nu)\|_{L^2(\mu)}.$$

- 4 Now we define

$$d_{\text{HK}, \mu, \text{lin}}(\mu_1, \mu_2) = \|\text{Log}_{\text{HK}}(\mu; \mu_1) - \text{Log}_{\text{HK}}(\mu; \mu_2)\|_{L^2(\mu)}.$$

- 5 Linear embedding map:

$$P_{\text{HK}, \mu, \text{lin}}(\mu_i) = \text{Log}_{\text{HK}}(\mu; \mu_i).$$

- 6 **Linear Hellinger–Kantorovich Assumption:**

$$d_{\text{HK}}(\mu_1, \mu_2) \approx d_{\text{HK}, \mu, \text{lin}}(\mu_1, \mu_2) = \|P_{\text{HK}, \mu, \text{lin}}(\mu_1) - P_{\text{HK}, \mu, \text{lin}}(\mu_2)\|_{L^2(\mu)}.$$

- 1 Solve the Kantorovich formulation to find π^* (e.g. Sinkhorn's algorithm)

$$d_{\text{HK}}^2(\mu, \nu) = \inf_{\pi \in \mathcal{M}_+(\Omega^2)} \left\{ \int_{\Omega^2} c \, d\pi + \text{KL}(P_{1\#}\pi|\mu) + \text{KL}(P_{2\#}\pi|\nu) \right\}.$$

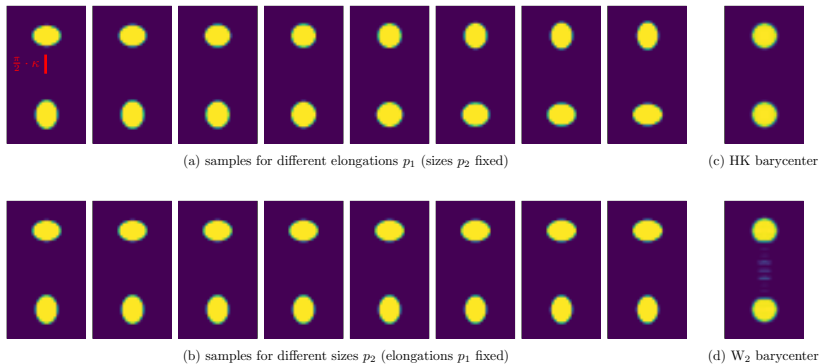
- 2 Extract T^* the optimal Monge map from $\pi^* = (\text{Id} \times T^*)_{\#}\tilde{\mu}$ and the densities u, w .
- 3 Compute the velocity and growth maps at time $t = 0$, i.e. v_0, α_0 using the previous theorem

$$d_{\text{HK}}^2(\mu, \nu) = \int_{\Omega} \left(\|v_0\|^2 + \frac{1}{4}(\alpha_0)^2 \right) d\mu.$$

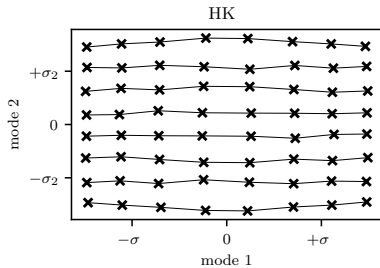
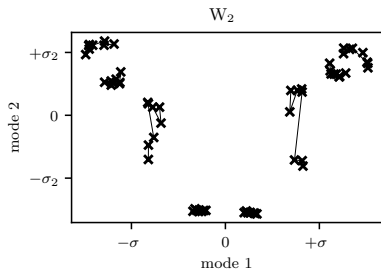
Road map:

$$\nu \mapsto \pi^* \mapsto (T^*, u, w) \mapsto (v_0, \alpha_0).$$

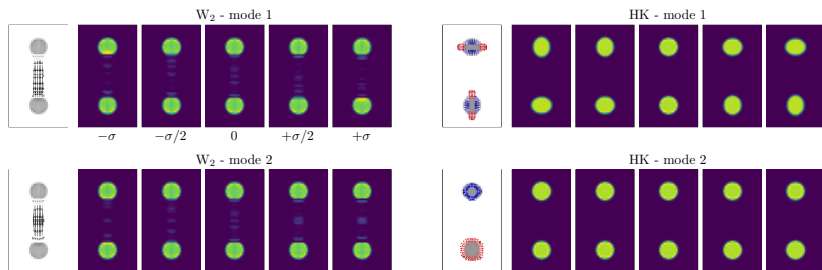
A Toy Example: Data and Barycentres



A Toy Example: 2D PCA Projection

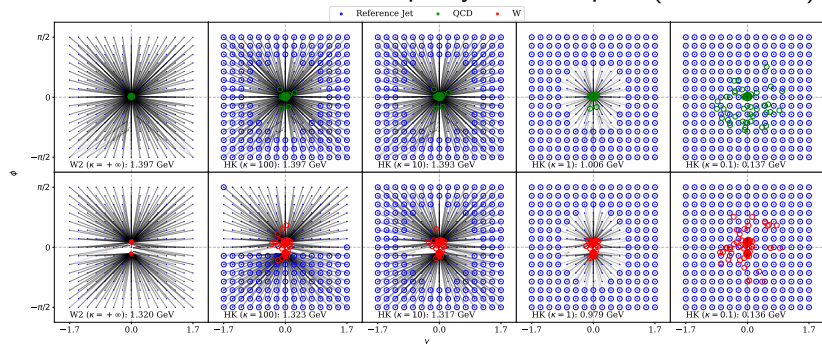


A Toy Example: Dominant Eigenmodes

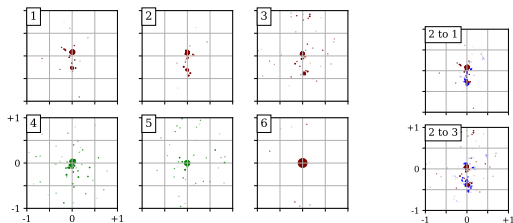
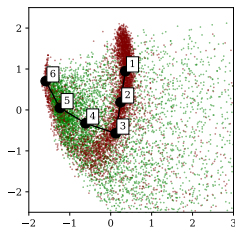
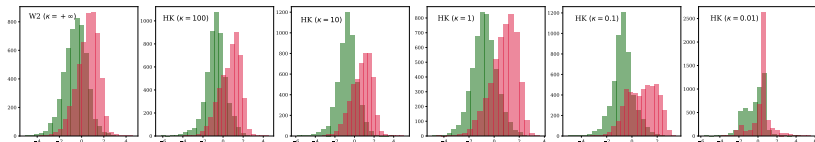


For each mode, the quiver plot on the left shows the initial velocity field v_0 , for HK the color of the arrows encodes α_0 (blue means decrease, red increase of mass). The five images on the right visualize the exponential map evaluated between $-\sigma$ and σ where σ denotes the standard deviation along the considered mode.

Aim: Jet tagging. In particular, can we label W boson jets and QCD (quark or gluon) jets from a simulated dataset of particle collider events observed in the rapidity-azimuth plan (i.e. $\Omega \subset \mathbb{R}^2$).



Collider Events: LDA and PCA



Collider Events: Labelling

Figure: Results for the W vs. QCD jet tagging task using LDA, kNN and SVM on the (unbalanced) linearized OT embeddings for various length scale parameters κ ($\kappa = +\infty$ denotes balanced the Wasserstein distance).

length scale κ		$+\infty$	100	10	5	1	0.7	0.5	0.3	0.1	0.05	0.01
LDA	AUC	0.694	0.733	0.746	0.747	0.752	0.751	0.748	0.760	0.765	0.763	0.642
	TPR	0.684	0.684	0.703	0.721	0.724	0.740	0.736	0.692	0.704	0.731	0.770
	FPR	0.296	0.218	0.211	0.226	0.220	0.239	0.239	0.171	0.174	0.205	0.486
	run time	several seconds										
kNN	AUC	0.821	0.818	0.819	0.818	0.829	0.841	0.849	0.847	0.821	0.772	0.671
	TPR	0.771	0.763	0.768	0.763	0.760	0.791	0.798	0.809	0.821	0.783	0.733
	FPR	0.128	0.127	0.130	0.126	0.102	0.110	0.100	0.114	0.181	0.238	0.390
	hyperpar. k	30	20	30	20	10	20	10	20	10	10	30
run time	1.5 hours											
SVM	AUC	0.842	0.842	0.842	0.841	0.849	0.851	0.856	0.853	0.845	0.806	0.694
	TPR	0.817	0.819	0.817	0.819	0.823	0.829	0.832	0.829	0.788	0.741	0.787
	FPR	0.133	0.134	0.134	0.137	0.126	0.127	0.120	0.124	0.099	0.128	0.401
	hyperpar. C	1	1	1	1	1	1	1	1	1	10	10
hyperpar. γ	100	100	100	100	100	100	100	100	100	1000	1000	100000
run time	5 hours											

- 1 Wang, Slepčev, Basu, Ozolek and Rohde, *A Linear Optimal Transportation Framework for Quantifying and Visualizing Variations in Sets of Images*, International Journal of Computer Vision 101(2):254–269, 2013.
- 2 Kolouri, Park, T., Slepčev and Rohde, *Optimal Mass Transport: Signal Processing and Machine-Learning Applications*, IEEE Signal Processing Magazine, 34(4):43-59, 2017.
- 3 Gangbo, Li, Osher and Puthawala, *Unnormalized Optimal Transport*, preprint arXiv:1902.03367, 2019.
- 4 Lee, Lai, Li and Osher, *Generalized Unnormalised Optimal Transport and its Fast Algorithms*, preprint arXiv:2001.11530, 2020.
- 5 Chizat, Peyré, Schmitzer and Vialard, *Unbalanced Optimal Transport: Dynamic and Kantorovich Formulations*, Journal of Functional Analysis, 274(11):3090-3123, 2018.
- 6 Chizat, Peyré, Schmitzer and Vialard, *An Interpolating Distance Between Optimal Transport and Fisher–Rao Metrics*, Foundations of Computational Mathematics, 18(1):1-44, 2018a.
- 7 Kondratyev, Monsaingeon and Vorotnikov, *A new optimal transport distance on the space of finite Radon measures*, Advances in Differential Equations, 21:1117–1164, 2016.

- 8 Liero, Mielke and Savaré, *Optimal Entropy-Transport Problems and a New Hellinger–Kantorovich Distance Between Positive Measures*, *Inventiones Mathematicae*, 211(3):969-1117, 2018.
- 9 Cai, Cheng, Schmitzer, T., *The Linearized Hellinger–Kantorovich Distance*, arxiv:2102.08807, 2021.
- 10 Park and T., *Representing and Learning High Dimensional Data with the Optimal Transport Map from a Probabilistic Viewpoint*, CVPR, 2018.

People worry that computers will get too smart and take over the world, but the real problem is that they're too stupid and they've already taken over the world.

— Pedro Domingos